Angewandte Zuschriften

Hydrogen-Evolution Reaction

Deutsche Ausgabe: DOI: 10.1002/ange.201504376
Internationale Ausgabe: DOI: 10.1002/anie.201504376

Coupling Mo_2C with Nitrogen-Rich Nanocarbon Leads to Efficient Hydrogen-Evolution Electrocatalytic Sites

Yipu Liu, Guangtao Yu, Guo-Dong Li, Yuanhui Sun, Tewodros Asefa, Wei Chen,* and Xiaoxin Zou**

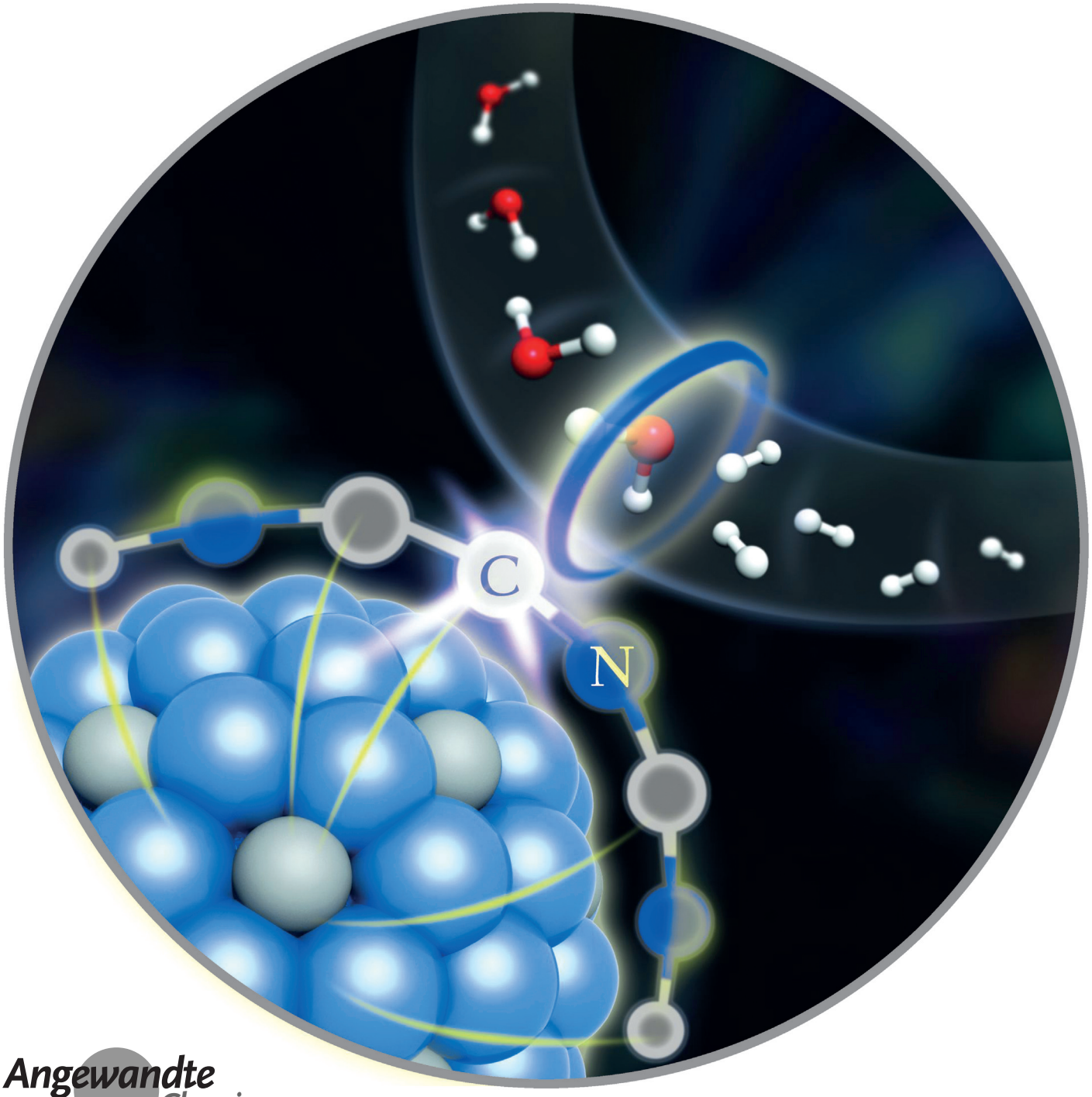

Angewandte Chemie

Abstract: *In our efforts to obtain electrocatalysts with improved activity for water splitting, meticulous design and synthesis of the active sites of the electrocatalysts and deciphering how exactly they catalyze the reaction are vitally necessary. Herein, we report a one-step facile synthesis of a novel precious-metal-free hydrogen-evolution nanoelectrocatalyst, dubbed Mo_2C@NC that is composed of ultrasmall molybdenum carbide (Mo_2C) nanoparticles embedded within nitrogen-rich carbon (NC) nanolayers. The Mo_2C@NC hybrid nanoelectrocatalyst shows remarkable catalytic activity, has great durability, and gives about 100 % Faradaic yield toward the hydrogen-evolution reaction (HER) over a wide pH range (pH 0–14). Theoretical calculations show that the Mo_2C and N dopants in the material synergistically co-activate adjacent C atoms on the carbon nanolayers, creating superactive nonmetallic catalytic sites for HER that are more active than those in the constituents.*

With an annual production of approximately 500 billion cubic meters, hydrogen (H_2) is one of the most important industrial feedstocks, currently widely used for petroleum refining and ammonia synthesis. This scenario is likely to change further, with hydrogen's potential to serve as a renewable alternative to fossil fuels in the future, and the surge of research on it as a result. However, current industrial production of H_2 primarily involves fossil fuels (e.g., natural gas),[1] which, needless to say, generate the greenhouse gas CO_2. Thus, more effort is needed to develop cleaner and sustainable hydrogen-production methods involving renewable energy-coupled electrocatalytic water splitting and photo(electro)chemical water splitting.[1,2]

At the heart of these efforts, and challenges therein, lies the design and synthesis of the right electrocatalysts for the reactions involved in water splitting. Although Pt-based materials are very active electrocatalysts for the hydrogen-evolution reaction (HER), Pt-free electrocatalysts, based on transition metals such as Mo, W, and Co, are preferable as they are more sustainable due to their low cost and high abundance.[1,3]

[*] Y. Liu,[+] Prof. G.-D. Li, Prof. X. Zou
State Key Laboratory of Inorganic Synthesis and Preparative Chemistry, International Joint Research Laboratory of Nano-Micro Architecture Chemistry, College of Chemistry, Jilin University
Changchun 130012 (P.R. China)
E-mail: xxzou@jlu.edu.cn
Prof. G. Yu,[+] Y. Sun, Prof. W. Chen
Institute of Theoretical Chemistry, International Joint Research Laboratory of Nano-Micro Architecture Chemistry, Jilin University
Changchun 130023 (P.R. China)
E-mail: xychwei@gmail.com
Prof. T. Asefa
Department of Chemistry and Chemical Biology & Department of Chemical and Biochemical Engineering
Rutgers, The State University of New Jersey
Piscataway, NJ 08854 (USA)
E-mail: tasefa@rci.rutgers.edu
[+] These authors contributed equally to this work.

Supporting information for this article is available on the WWW under http://dx.doi.org/10.1002/anie.201504376.

Owing to their similar d-band electronic density-of-state to that of Pt, high electrical conductivity, and optimal hydrogen-adsorption properties, transition-metal carbides, especially molybdenum and tungsten carbides, had long been expected to be effective non-Pt electrocatalysts for HER.[4] This was realized first in 2012, with the report by the Hu group that commercially available molybdenum carbide microparticles (com-Mo_2C) show good catalytic activity toward HER.[5] Since then, fine structural optimization of molybdenum carbide catalysts at the nanoscale has been actively pursued, and recent efforts have begun to bear more fruits.[6–9] However, in all of the molybdenum carbide HER nanocatalysts reported to date, including those containing nanocarbons,[8,9] the active sites have been considered to be present only on the surfaces of the molybdenum carbides, and the materials' overall catalytic activity has been shown to increase only by increasing the density of these active sites by nanostructuring. Moreover, although some molybdenum carbide/nanocarbon hybrid materials containing dopants have generally been found to have higher catalytic activity,[6a,8] the effect of dopants and the molybdenum carbide/nanocarbon interface on the materials' catalytic activity remains ambiguous.

Herein, we report a facile, one-step synthetic route that leads to a novel precious-metal-free HER electrocatalyst composed of ultrasmall molybdenum carbide (Mo_2C) nanoparticles embedded within nitrogen-rich carbon (NC) nanolayers (Figure 1 A). We also show that the Mo_2C@NC hybrid material exhibits an unprecedented high electrocatalytic activity for HER under acidic, neutral, or basic conditions alike. To the best of our knowledge, this is the first time that a Mo_2C-based material is shown to serve as an efficient HER electrocatalyst over a wide pH range. Theoretical calculations show that the Mo_2C acts as electron donor for the adjacent C atoms in the carbon nanolayers, whereas the N-dopant atoms function as electron acceptor; this synergy between Mo_2C and N dopants is found to yield unprecedented, superactive nonmetallic catalytic sites on the carbon nanolayers that are more active than those in Mo_2C.

The Mo_2C@NC was synthesized by a simple one-step thermal treatment in Ar atmosphere of homogeneously mixed ammonium molybdate and dicyandiamide (Figures 1 A and S1; see the Supporting Information, SI, for details). The use of dicyandiamide is crucial in the synthesis of Mo_2C@NC as it undergoes carbonization and helps the deoxygenation of ammonium molybdate, leading to the in situ generation of the nanocarbon species coupled with the Mo_2C nanoparticles. The most optimal pyrolysis temperature and weight ratio (ammonium molybdate/dicyandiamide) were found to be 800 °C and 1:2, respectively, and this condition gave a material that is denoted hereafter as Mo_2C@NC, unless indicated otherwise.

The structure and composition of the Mo_2C@NC were studied by powder X-ray diffraction (XRD), Raman, and X-ray photoelectron spectroscopy (XPS; Figure S2). The results showed that Mo_2C@NC was composed of β-phase of Mo_2C and N-rich carbon with N/C atomic ratio of about 1:5. Transmission electron microscopy (TEM) images (Figure 1 B,C) showed that Mo_2C@NC consisted of uniformly

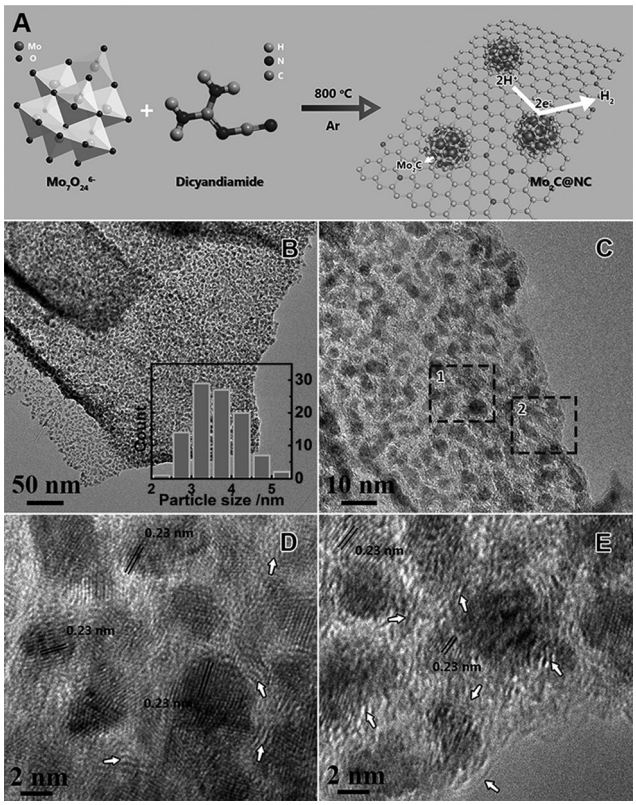

Figure 1. A) Illustration of the synthesis and the structure of Mo_2C@NC. B,C) TEM images of Mo_2C@NC. Inset in (B) displays particle size distribution of the Mo_2C nanoparticles. D,E) HRTEM images of the areas 1 and 2, respectively, in (C). The distance between the lines is 0.23 nm in all cases.

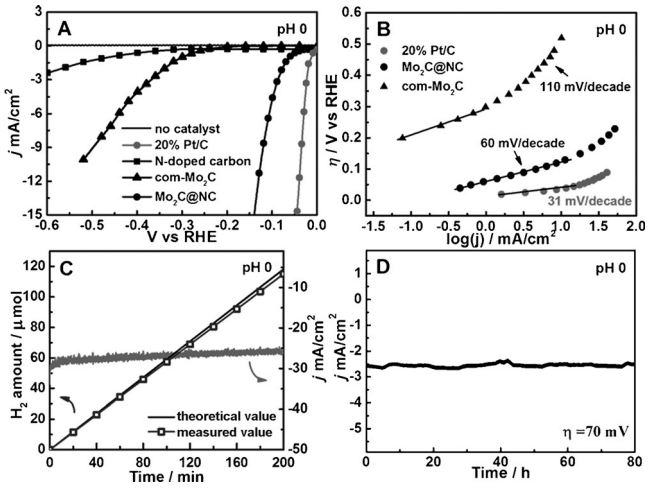

Figure 2. A) Steady-state current density as a function of applied voltage during HER at pH 0 over 20 wt% Pt/C, N-doped carbon, com-Mo_2C, and Mo_2C@NC. B) Tafel plots for the HER over 20 wt% Pt/C, com-Mo_2C, and Mo_2C@NC. C) Electrocatalytic efficiency of hydrogen production over Mo_2C@NC at a current density of ca. 25 mA cm^{-2}, measured for 200 min. D) Current density vs. time (*I*–*t*) curve of HER over Mo_2C@NC at $\eta = 70$ mV over 80 h-long electrocatalytic reaction.

shaped nanoparticles with an average size of 3.6 nm that are encapsulated within lamellar carbon matrices. Elemental mapping of Mo_2C@NC (Figure S3) revealed that the Mo, N, and C atoms were homogeneously distributed over the entire material, suggesting that the Mo_2C nanocrystals were uniformly distributed within the carbon matrices. High-resolution TEM images (Figure 1 D and E) further corroborated that the Mo_2C nanoparticles were wrapped in carbon nanolayers. The observed lattice spacing on carbide nanoparticles was ca. 0.23 nm, which corresponds to the distance between the (101) crystal planes of β-Mo_2C phase. In addition, some crystalline nanocarbons with 2–4 layers of carbon atoms, with a lattice spacing of ca. 0.34 nm, were seen around the carbide nanoparticles (as indicated with white arrows in Figure 1 D and E), although amorphous carbon still dominated the lamellar carbon matrix around the nanoparticles.

The electrocatalytic activity of Mo_2C@NC for HER in acidic (pH 0), neutral (pH 7), or basic (pH 14) media was then evaluated (SI). For comparison, the electrocatalytic activity of commercially available Mo_2C (com-Mo_2C), N-doped carbon (NC), and Pt/C (20 wt%) was also measured by using the same weight of samples in all the cases.

First, the electrocatalytic activity of the materials in acidic media was investigated. As shown in Figure 2 A, the N-doped carbon and com-Mo_2C produced a current density of 1 mA cm^{-2} at an overpotential (η) of 360 and 300 mV, respectively, whereas Mo_2C@NC gave the same current density at a much lower η of 60 mV. In line with this result, Mo_2C@NC gave a smaller Tafel slope (60 mV/decade) than com-Mo_2C (110 mV/decade; Figure 2 B). Moreover, Mo_2C@NC showed a higher exchange current density (9.6×10^{-2} mA cm^{-2}) than com-Mo_2C (1.2×10^{-3} mA cm^{-2}). Hence, Mo_2C@NC can be said to be a much better electrocatalyst for HER than either N-doped carbon or com-Mo_2C. Furthermore, Mo_2C@NC afforded a current density of 10 mA cm^{-2} (i.e., the current density expected for a 12.3% efficient solar water-splitting device) at relatively low η of 124 mV. Thus, the results overall demonstrated that Mo_2C@NC was an excellent water-splitting electrocatalyst. In fact, Mo_2C@NC's catalytic activity is either comparable with or superior to the best Mo_2C-based HER electrocatalysts reported so far (Table S1).

Figure 2 C compares the graphs of the amount of H_2 generated from the HER over Mo_2C@NC versus the theoretically possible H_2 that can be evolved from electrochemical HER. Mo_2C@NC clearly shows not only a stable hydrogen-evolution rate but also a rate (34.5 μmol h^{-1}) that is very close to the theoretically achievable value. In other words, the result demonstrates that Mo_2C@NC gives about 100% Faradaic yield and has excellent stability in HER. Mo_2C@NC actually retained its activity and morphology even after 80 h-long electrocatalytic HER (Figures 2 D and S4).

Until now most Mo_2C-based HER electrocatalysts have been found to work well only in acidic media.[5–9] However, many water–alkali and chloro–alkali HER electrolyzers need active and durable catalysts that can operate in basic environment, and many microbial electrolysis cells typically need electrocatalysts that can function well in neutral media.[10] As shown in Figure 3 A and B, our Mo_2C@NC exhibited good electrocatalytic activity toward HER both in

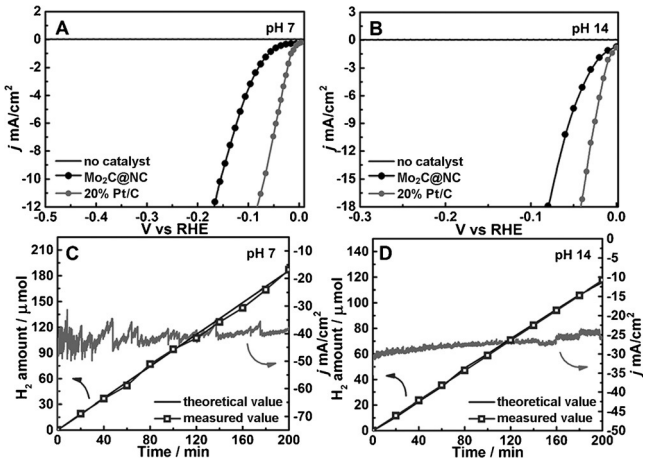

Figure 3. A,B) Steady-state current density as a function of applied voltage at pH 7 and pH 14 over 20 wt% Pt/C and Mo_2C@NC. C,D) Efficiency of hydrogen production over Mo_2C@NC at pH 7 and pH 14. The values of current density are all normalized with the surface area of the GCE.

neutral and basic media, affording a current density of 10 mA cm^{-2} at ultrasmall overpotentials of 156 and 60 mV, respectively. It is worth noting that such high catalytic activity in neutral or basic media has never been achieved for Mo_2C-based catalysts before (Table S1), and Mo_2C@NC's activity in neutral and basic media was comparable to those of the best non-Mo_2C-based, noble metal-free HER electrocatalysts (Tables S2 and S3). Additionally, Mo_2C@NC showed excellent stability and about 100% Faradaic yield in both media (Figures 3C,D and S5). Overall these results clearly indicate that the Mo_2C@NC is a highly versatile, efficient HER electrocatalyst for a wide pH range (pH 0–14).

To uncover the interplay between the structures and the catalytic activity of the materials, a series of relevant samples was prepared by varying the weight ratio of the precursors (i.e., ammonium molybdate/dicyandiamide) and the pyrolysis temperature, and their properties were examined (Figure 4). Note that Mo_2C materials form only at or above 800 °C; so, by maintaining the temperature constant (800 °C), but using 1:1 and 1:3 ratios of the precursors, two different materials that were labeled as s-800-1/1 and s-800-1/3, respectively, were synthesized. Additionally, by keeping the ratios of the precursors constant (1:2), but using 900 and 1000 °C, two more materials denoted as s-900-1/2 and s-1000-1/2, respectively, were obtained. The Mo_2C@NC discussed above, which was made from a 1:2 ratio of precursors at 800 °C, was denoted as s-800-1/2 here for comparison.

Sample s-800-1/1 was found to have Mo_2C microparticles without carbon residue, possibly due to the relatively low dicyandiamide used for its synthesis, whereas s-800-1/3 was found to have N-doped carbon-encapsulated MoC nanoparticles with ca. 3.2 nm in size (Figures S6 and S7). Note that s-800-1/2 contained Mo_2C nanoparticles ($\approx$3.6 nm) embedded within N-doped carbon nanolayers. Thus, the results suggest that the carbon matrices prevent the Mo_2C nanoparticles from coalescence/sintering at high temperatures. The materials' catalytic activity (Figure 4A) was found to decrease in the order of s-800-1/2 > s-800-1/3 $\gg$ s-800-1/1, indicating that the small-size carbide particles were important for the material's catalytic activity. In view of the fact that both s-800-1/2 and s-800-1/3 had carbon-encapsulated carbide nanoparticles with similar size, the higher catalytic activity of s-800-1/2 might be due to the higher density of N dopants in it (Figure 4B).

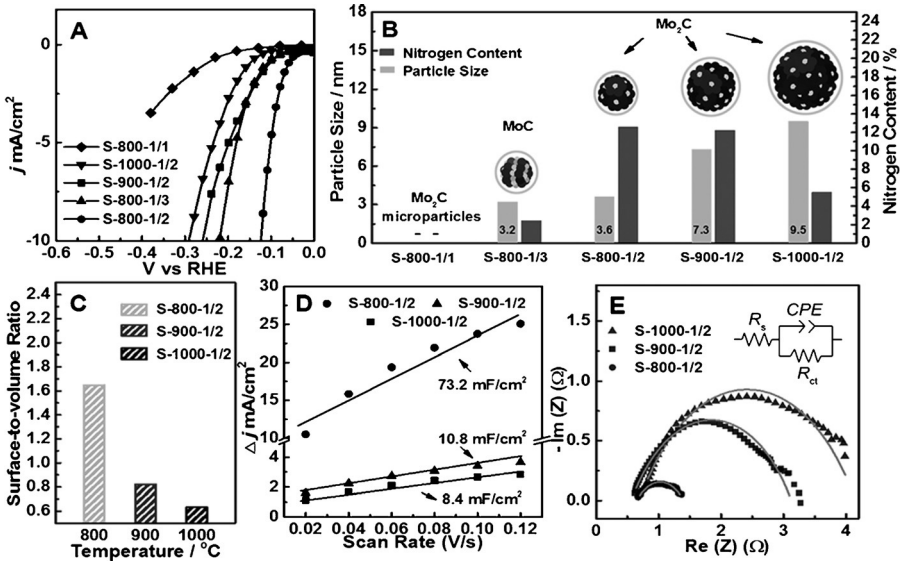

Figure 4. A) Comparison of the catalytic activities of five samples synthesized at different temperatures and ratios of starting materials. B) Comparison of particle size and N/C atomic ratio for the five samples prepared under different conditions. C) The calculated surface-to-volume ratios based on particle sizes of the samples. D) The difference in current density (j) between the anodic and cathodic sweeps (Δj) versus scan rate; the slope of the fitting line is used for determination of the double-layer capacitance (C_{dl}). E) Nyquist plots obtained by electrochemical impedance spectroscopy (EIS) for s-800-1/2, s-900-1/2, and s-1000-1/2. The data are fitted to the simplified equivalent circuit shown in the inset, and the fitting results are plotted as solid traces.

On the other hand, the materials s-800-1/2, s-900-1/2, and s-1000-1/2 were all found to have carbon-encapsulated Mo_2C nanoparticles, with increasing particle size and decreasing order of N-dopant density as their pyrolysis temperature was increased (Figures 4B, S8, and S9). These structural variations correlated well with the catalytic activities of the materials, which decreased in the order of 800-1/2 > s-900-1/2 > s-1000-1/2, Figure 4A. Accordingly, the surface-to-volume ratio of

carbon nanoparticles and the electrochemical surface area for the obtained samples (which is s-800-1/2 > s-900-1/2 > s-1000-1/2, Figure 4C and D) were both found to be directly related to the material's catalytic activity. Additionally, electrochemical impedance spectra (Figure 4E) showed that s-800-1/2 had a much lower Faradaic impedance than s-900-1/2 and s-1000-1/2, indicating that the electron transfer rates in HER was much faster in the presence of s-800-1/2 than the latter two.

To gain further insight into the high electrocatalytic activity of the Mo_2C@NC material, we additionally performed density functional theory (DFT) calculations by constructing the correlative theoretical models (Figure S10 and Tables S4 and S5). It is well known that the adsorption free energy of H ($\Delta G(H^*)$) can serve as a good measure for the activity of a catalytic material for HER, for which a catalyst that gives $\Delta G(H^*) \approx 0$ is considered a good candidate for HER.[11] Our calculations of the $\Delta G(H^*)$ value on the surfaces of Mo_2C@NC are described in Figure 5 and Table S5. For comparison, a similar calculation

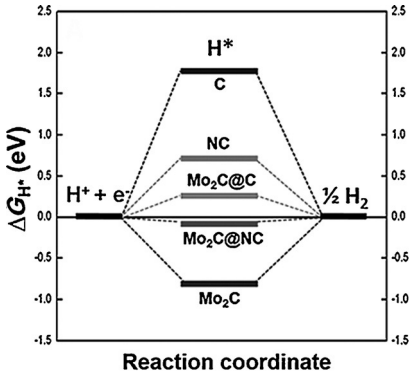

Figure 5. The calculated free-energy diagram of HER at equilibrium potential for five possible structures, namely Mo_2C@NC, Mo_2C@C, Mo_2C, C, and NC.

was conducted for carbon-layer-encapsulated Mo_2C nanoparticles (Mo_2C@C), Mo_2C, carbon layer (C), and N-rich carbon layer (NC). As illustrated in Figure 5, Mo_2C@NC gave a much smaller $\Delta G(H^*)$ value than its constituents (i.e., C, NC, and Mo_2C), indicating that the hybrid nanomaterial possessed a higher catalytic activity for HER. This is in good agreement with the experimental results discussed above. Furthermore, $\Delta G(H^*)$ of Mo_2C@NC was much smaller than that of Mo_2C@C, indicating that the N dopants introduced in the carbon nanolayers further enhanced the electrocatalytic performance of the material. In fact, the carbon atoms adjacent to the N dopants were found to be the most electrocatalytically active sites in Mo_2C@NC (see SI).

The presence of synergistic effects between the Mo_2C nanoparticles and the N dopants in Mo_2C@NC were further explored by comparing the difference in charge density ($\Delta\rho$) between Mo_2C@NC and Mo_2C@C (Figure S11). An electron-transfer process from Mo_2C to the carbon layer in Mo_2C@C was evident from the observed blue color on all of the carbon atoms in the corresponding $\Delta\rho$ plot. However, besides this electron-transfer process, electron transfer from the adjacent C atoms (those shown in yellow) to N atoms was simultaneously seen in Mo_2C@NC. These results revealed the strong electron-withdrawing features of N dopants in the material. This, in turn, could induce a complex electron-transfer process ($Mo_2C \rightarrow C \rightarrow N$) in Mo_2C@NC, making the neighboring C atoms to play dual roles both as electron acceptors and electron donors. This result reinforces the presence of the synergy between Mo_2C and N dopants, rendering unprecedented catalytic activity to the C atoms adjacent to N atoms in the carbon layer and making Mo_2C@NC a highly efficient HER catalyst.

In conclusion, a precious-metal-free HER electrocatalyst containing ultrasmall molybdenum carbide (Mo_2C) nanoparticles embedded in nitrogen-rich carbon (NC) nanolayers has been synthesized in one step from inexpensive precursors. Theoretical studies have revealed a synergistic effect between Mo_2C and N dopants that yield superactive nonmetallic HER catalytic sites on the carbon nanolayers.

Acknowledgements

X.Z. and W.C. appreciate the financial support from the NSFC (21371070, 21401066, 21103065, and 21373099), Jilin Province Science and Technology Development Project (20150520003JH), and the Ministry of Education of China (20110061120024 and 20130061110020). T.A. gratefully acknowledges financial support by the NSF (NSF CBET-1134289). This work was also supported by the Graduate Innovation Fund of Jilin University (2015010).

Keywords: catalytically active site · composite material · electrocatalysis · molybdenum carbide · water splitting

How to cite: *Angew. Chem. Int. Ed.* **2015**, *54*, 10752–10757
Angew. Chem. **2015**, *127*, 10902–10907

[1] X. Zou, Y. Zhang, *Chem. Soc. Rev.* **2015**, DOI: 10.1039/c4cs00448e.
[2] a) J. R. Swierk, T. E. Mallouk, *Chem. Soc. Rev.* **2013**, *42*, 2357; b) Y. Jiao, Y. Zheng, M. Jaroniec, S. Z. Qiao, *Chem. Soc. Rev.* **2015**, *44*, 2060; c) X. Zou, X. Huang, A. Goswami, R. Silva, B. R. Sathe, E. Mikmeková, T. Asefa, *Angew. Chem. Int. Ed.* **2014**, *53*, 4372; *Angew. Chem.* **2014**, *126*, 4461.
[3] a) M. S. Faber, S. Jin, *Energy Environ. Sci.* **2014**, *7*, 3519; b) J. D. Benck, T. R. Hellstern, J. Kibsgaard, P. Chakthranont, T. F. Jaramillo, *ACS Catal.* **2014**, *4*, 3957.
[4] For example see: a) Y. Zhao, K. Kamiya, K. Hashimoto, S. Nakanishi, *Angew. Chem. Int. Ed.* **2013**, *52*, 13638; *Angew. Chem.* **2013**, *125*, 13883; b) C. Wan, Y. N. Regmi, B. M. Leonard, *Angew. Chem. Int. Ed.* **2014**, *53*, 6407; *Angew. Chem.* **2014**, *126*, 6525; c) Y. Liu, G.-D. Li, L. Yuan, L. Ge, H. Ding, D. Wang, X. Zou, *Nanoscale* **2015**, *7*, 3130.
[5] H. Vrubel, X. Hu, *Angew. Chem. Int. Ed.* **2012**, *51*, 12703; *Angew. Chem.* **2012**, *124*, 12875.
[6] a) L. Liao, S. Wang, J. Xiao, X. Bian, Y. Zhang, M. D. Scanlon, X. Hu, Y. Tang, B. Liu, H. H. Girault, *Energy Environ. Sci.* **2014**, *7*, 387; b) Y. Zhao, K. Kamiya, K. Hashimoto, S. Nakanishi, *J. Am. Chem. Soc.* **2015**, *137*, 110; c) H. B. Wu, B. Y. Xia, L. Yu, X.-Y. Yu, X. W. Lou, *Nat. Commun.* **2015**, DOI: 10.1038/ncomms7512.
[7] a) K. Zhang, Y. Zhao, D. Fu, Y. Chen, *J. Mater. Chem. A* **2015**, *3*, 5783; b) K. Xiong, L. Li, L. Zhang, W. Ding, L. Peng, Y. Wang, S. Chen, S. Tan, Z. Wei, *J. Mater. Chem. A* **2015**, *3*, 1863.

[8] D. H. Youn, S. Han, J. Y. Kim, J. Y. Kim, H. Park, S. H. Choi, J. S. Lee, *ACS Nano* **2014**, *8*, 5164.
[9] W. Cui, N. Cheng, Q. Liu, C. Ge, A. M. Asiri, X. Sun, *ACS Catal.* **2014**, *4*, 2658.
[10] R. Subbaraman, D. Tripkovic, D. Strmcnik, K.-C. Chang, M. Uchimura, A. P. Paulikas, V. Stamenkovic, N. M. Markovic, *Science* **2011**, *334*, 1256.
[11] a) Y. Zheng, Y. Jiao, Y. Zhu, L. H. Li, Y. Han, Y. Chen, A. Du, M. Jaroniec, S. Z. Qiao, *Nat. Commun.* **2014**, *5*, 3783; b) J. Deng, P. Ren, D. Deng, L. Yu, F. Yang, X. Bao, *Energy Environ. Sci.* **2014**, *7*, 1919.

Received: May 13, 2015
Published online: July 23, 2015

